PNNL-28595

Pacific Northwest
NATIONAL LABORATORY

Photofission Validation Measurements for Active Interrogation Standards

April 2019

GA Warren RT Kouzes

U.S. DEPARTMENT OF ENERGY

Prepared for the U.S. Department of Energy
under Contract DE-AC05-76RL01830

DISCLAIMER

PACIFIC NORTHWEST NATIONAL LABORATORY
operated by
BATTELLE
for the
UNITED STATES DEPARTMENT OF ENERGY
under Contract DE-AC05-76RL01830

Printed in the United States of America

Available to DOE and DOE contractors from the Office of Scientific and Technical Information,
P.O. Box 62, Oak Ridge, TN 37831-0062
www.osti.gov
ph: (865) 576-8401
fax: (865) 576-5728
email: reports@osti.gov

Available to the public from the National Technical Information Service
5301 Shawnee Rd., Alexandria, VA 22312
ph: (800) 553-NTIS (6847)
or (703) 605-6000
email: info@ntis.gov
Online ordering: http://www.ntis.gov

PNNL-28595

Photofission Validation Measurements for Active Interrogation Standards

April 2019

GA Warren RT Kouzes

Prepared for
the U.S. Department of Energy
under Contract DE-AC05-76RL01830

Pacific Northwest National Laboratory
Richland, Washington 99352

Executive Summary

PNNL has been developing technical standards for the detection of special nuclear material (SNM) in cargo containers using active interrogation approaches. Since the use of kilogram-scale quantities of SNM is impractical for standards testing, the work focused on designing surrogates that provided similar signature as the SNM. There are many active interrogation approaches to detect SNM; the standards development considered photofission, differential die-away and nuclear resonance fluorescence. Of these approaches, photofission currently carries the most interest. However, uncertainties in the photofission cross sections are as large as 50%, so that validation measurements are necessary to provide confidence that the surrogate will perform similarly to the SNM. This document describes approaches for conducting those validation measurements as well as provides a rough order-of-magnitude cost estimate for performing them.

Photofission provides many observables for the detection of SNM. The standards development considered prompt neutrons, delayed neutrons and delayed gamma rays as possible detected particles. The surrogates, which consist primarily of depleted uranium (DU), were designed to reproduce the strength of these particles for a targeted quantity of 2 kg of HEU. Different surrogates are required for different measurement approaches because of the difference in cross section between ^{235}U and ^{238}U. For the standards validations, the relative strength of the detected particles for HEU and DU must be measured.

To avoid measurements with kilogram-sized SNM, the validation approach is focused on two comparisons. In the first comparison, the relative rates for approximately 10 g samples of DU and HEU will be measured. This comparison will provide the basis for validating the relative strength of the detected particles for HEU and DU. In the second comparison, the relative rates for the approximately 10 g and 1 kg sample of DU will be measured. This comparison will enable the validation of secondary processes that occur after photofission that impact the measurement for kilogram-scale samples. For instance, for 2 kg of HEU, as much as 50% of the fission induced in the sample is induced from fission neutrons generated through photofission.

There is a limited range of facilities in the U.S. that have both the necessary accelerator capability and the ability and willingness to handle SNM. Two such facilities, the Idaho Accelerator Center at Idaho State University and the Nuclear Engineering Program at the University of Michigan, have both expressed an interest in participating in such measurements. Both would need to amend their licensing to handle the 10 g of HEU proposed for these measurements.

The rough order-of-magnitude cost estimate for all three validation measurements is $1.1M, spread over three years. Each of the three measurements could be performed separately, at approximately one-third of that cost. There are a number of critical assumptions in these cost estimate that will need to be confirmed before a more reliable cost estimate can be established.

PNNL will manage the effort to ensure that the overall objective of the validation measurements can be achieved and will fabricate the 10 g samples of HEU and DU. Most the labor for the measurements will be provided by two collaborating universities as research opportunities for students. The successful completion of these validation measurements will reduce the uncertainties in the proposed standards from about 50% to 5%. The measurements would also provide some much-needed nuclear data on photofission.

Acronyms and Abbreviations

AI	active interrogation
DU	depleted uranium
eV	electron Volt
ENDF	evaluated nuclear data file
HDPE	high-density polyethylene
HEU	highly enriched uranium
IAC	Idaho Accelerator Center
keV	kilo-electron volt
MeV	mega-electron volts
NRF	nuclear resonance fluorescence
Pu	plutonium
S/N	signal to noise
SNM	special nuclear material
XCOM	photon cross section database
Z	atomic number

Contents

Figures

Tables

1.0 Introduction

The detection of special nuclear material (SNM) in cargo is a challenge for passive radiation measurements that observe the radiation signatures spontaneously emitted by the SNM. Highly enriched uranium (HEU), for instance, emits very few neutrons and the strongest gamma rays are easily attenuated. Alternatively, cargo around the SNM may serve as shielding, reducing the observable signal strengths. For this reason, active interrogation techniques, where we broadly define active-interrogation as the use of energy external to a sample to probe the response of the sample, are being pursued for detection of SNM in cargo.

PNNL has been developing a proposed testing standard for systems designed to actively interrogate cargo containers (Kouzes et al. 2019). The primary challenge of testing under such a standard is that the objects that one wants to test against, kilogram-scale quantities of highly enriched uranium (HEU) and weapons-grade plutonium (WGPu), are not easily accessible to commercial vendors. As a result, much of the challenge of developing the standard involved developing suitable surrogates, such as depleted uranium (DU), that were more readily obtainable and provided a similar interrogation response as the targeted quantities of HEU and WGPu. Several different active interrogation approaches were considered such as photofission, nuclear resonance fluorescence and differential die-away. Of these approaches, the largest uncertainties, on the scale of 50%, occurred for the various photofission processes. These large uncertainties are due to the paucity of related photofission nuclear data and models. The report presents an experimental plan for conducting validation measurements for the photofission processes.

There is a wealth of possible observables from photofission that can be utilized for detection of SNM in cargo containers. There are prompt neutrons from photofission, where the proposed standard considers three different energy ranges for the neutrons, greater than 0.5 eV, greater than 1 MeV and greater than 3 MeV. The prompt photons are not considered because they are difficult to distinguish from the photons scattered off the target due to non-fission-related processes. There are delayed neutrons, which can be emitted up to several minutes after the fission. There are delayed photons, which can be emitted up to a couple of hours after the fission. For the delayed neutrons and photons, three different integration times of 1 ms to 0.1 s, 1 s, and 10 s were considered. Furthermore, delayed photons with more than 3 MeV energy were also considered. As will be discussed later, this time binning is likely not appropriate for how the interrogations will be conducted. The goal of the proposed validation measurements is to conduct a 5% measurement of the relative contribution of DU compared to HEU for these various signatures. In most cases, estimates show that this goal can be achieved in a reasonable amount of time, with beam times on the scale of a few days.

This paper presents the plan for validation measurements of a proposed standard for photofission active interrogation. This will ensure that the requirements in the standard are appropriate and achievable. This paper is organized into two additional sections, one focused on describing the count rate estimates for predicting how much measurement time is required, and one focused on estimated costs of the proposed experiments. Within the count rate section, discussions include choice of targets, detectors, and beam structure. Within the cost estimate section, discussion of alternatives facilities, such as the Idaho Accelerator Center at Idaho State University and the Nuclear Engineering program at the University of Michigan, are presented.

2.0 Estimated Count Rates

There are two extreme approaches for designing the validation measurements. First, one can conduct measurements with the kilogram-scale targeted SNM and related surrogates. Second, one can identify the processes in the current modeling that are poorly understood and focus on experiments to study those

specific processes. The former approach would involve extensive and expensive work at a national laboratory due to the kilogram-scale sizes of SNM involved but provide higher fidelity results for the standard. Likely, Idaho National Laboratory (INL) is the only national laboratory with the accelerators and material capable for conducting such measurements. Although INL does not currently have the capabilities to conduct these measurements, they have conducted similar measurements in the past and likely could conduct them in the future. We have assumed that the costs would be prohibitive for a measurement at INL, so we have focused on the second approach, which use much smaller quantities of SNM.

There are several parameters for estimating the count rates for the needed measurement to reduce the current uncertainties. The basic equation for calculating the count rates is

$$R = \phi I n \sigma \nu \epsilon N_{det} \frac{\Delta\Omega}{4\pi}, \quad (1)$$

where ϕ is the photon flux on the target per beam charge [γ/mC], I is the average beam current [mA], n is the areal density of the target [atoms/cm^2], σ is the cross section for the process of interest [cm^2], ν is the number of particles of interest generated per interaction [unitless], ϵ is the intrinsic efficiency [unitless], N_{det} is the number of detectors and $\Delta\Omega$ is the solid angle of the detector-target geometry [sr]. Each of these terms are discussed in the subsections below.

2.1 Targets

The primary concern for the validation is the strength of observables from photofission for DU compared to HEU. It is assumed that the *transport* of those observables, neutrons and photons of various energies and timings, through various materials, can be well-modeled with existing transport codes. However, the *production* of those observables via photofission are less well modeled, in part due to a lack of adequate nuclear data. This type of measurement is best performed with a thin sample of material to reduce the secondary scattering that may occur in the target. However, the secondary scattering in an extended target is important. For instance, even for photofission, up to one-half of the fissions that occur in a kg-sized HEU or DU from exposure to a photon beam are induced by neutrons created by the photon beam. In other words, for extended targets about half of the fissions in the target can be generated through secondary processes from the original photon beam. Thus, it is also important to study larger targets to allow for the increased probability of secondary scattering.

With these considerations, the validation measurements are designed with three different targets, a thin, small mass HEU target, a thin, small mass DU target, and a larger, thicker DU target. The mass of the HEU target is set to 10 g. Masses of HEU larger than 10 g have increased administrative overhead in dealing with safety, transportation and material licensing issues. The small DU target should match the HEU target to facilitate the comparison of the observed rates. The small targets are assumed to be square for these calculations. We propose for the larger DU target a 1 kg mass of DU, ideally in a solid sphere, although any solid geometry with approximately equal dimensions will be adequate; we assume a cube in the rate estimates. One kilogram is sufficient to test secondary scattering effects. Details of the proposed (metal) target materials can be found in Table 1.

Table 1. Proposed Target Materials.

	HEU	Small DU	Large DU
Mass [g]	10	10	1,000
Density [g/cm^3]	19.0	19.0	19.0
A [g/mole]	235.2	238	238
Thickness [mm]	1.0	1.0	37.5
Width [mm]	22.9	22.9	37.5
n [atoms/cm^2]	$4.9 \cdot 10^{21}$	$4.9 \cdot 10^{21}$	$1.8 \cdot 10^{23}$

2.2 Fission Rates

The rate that fissions and (γ, n) reactions occur in the target is a product of the bremsstrahlung photon beam energy distribution and the energy dependence of the photofission cross section. The bremsstrahlung photon beam energy distribution is determined through radiation transport modeling using the Geant4 framework (Agostinelli et al. 2003; Allison et al. 2006). The bremsstrahlung radiator consists of a 0.25 mm tungsten mounted on 10 mm thick copper. A lead collimator is applied to the bremsstrahlung beam. The bremsstrahlung beam energy distribution is expressed in units of photons/mC/msr/MeV, which assumes that the photon distribution is flat across the target. The photofission and (γ, n) cross sections are taken from ENDF/B-VII.1 (Chadwick et al. 2011). The bremsstrahlung distribution and cross sections are shown in Figure 1. To simplify the calculation, the cross sections up to 9 MeV are approximated as horizontally-offset exponential functions. To determine the solid angle of the target with respect to the beam, a distance between the radiator and the target of 3 m is assumed; the solid angles of the beam for the 10 g and 1,000 g targets are 0.058 and 0.156 msr, respectively. The products of these distributions, as well as factors including the target solid angle, are shown in

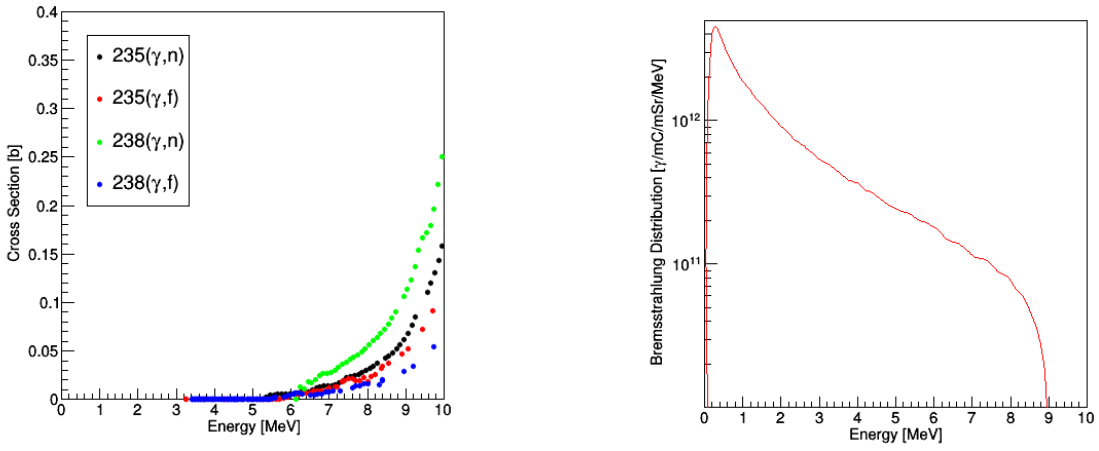

Figure 1. U cross sections (left) and bremsstrahlung photon distribution (right)

Table 2.

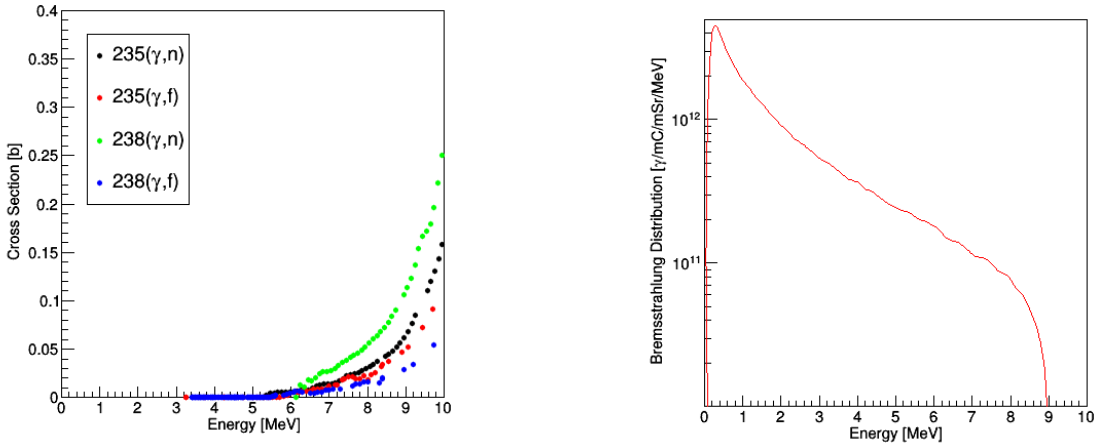

Figure 1. U cross sections (left) and bremsstrahlung photon distribution (right)

Table 2. Product of cross section of bremsstrahlung energy distribution for relevant processes

Reaction	Product	$\phi\sigma\left[\frac{cm^2}{mC}\right]$	
	$\left[b \cdot \frac{\gamma}{mC \cdot msr}\right]$	10 g Target	1,000 g Target
$^{235}U(\gamma,n)$	$1.91 \cdot 10^{9}$	$1.1 \cdot 10^{-16}$	N/A
$^{235}U(\gamma,f)$	$1.36 \cdot 10^{9}$	$7.9 \cdot 10^{-17}$	N/A
$^{238}U(\gamma,n)$	$3.07 \cdot 10^{9}$	$1.8 \cdot 10^{-16}$	$4.8 \cdot 10^{-15}$
$^{238}U(\gamma,f)$	$9.90 \cdot 10^{8}$	$5.8 \cdot 10^{-17}$	$1.5 \cdot 10^{-15}$

2.3 Detector Efficiencies and Solid Angles

The efficiencies of the detectors depend on the placement of the detectors to determine solid angle of the detector with respect to the target and the intrinsic efficiency of the detector. Both the type of the detector and the placement vary with the type of photofission observable, which are each discussed below. A summary of the efficiencies, as well as the number of detectors N_{det} for the count rate estimates, is shown in Table 3.

Table 3. Detector parameters for estimating count rate

Particle	ϵ	$\Delta\Omega/4\pi$	N_{det}
Prompt Neutrons	0.04	0.0022	4
Delayed Neutrons	0.054	0.028	6
Delayed Photons, all *E*	0.29	0.012	4
Delayed Photons, *E* > 3 MeV	0.13	0.012	4

2.3.1 Prompt Neutrons

The proposed standard allows for three different energy thresholds when counting fast neutrons, namely 0.5 eV, 1 MeV and 3 MeV. To design an experiment that is capable of simultaneously measuring these thresholds, we propose to conduct time-of-flight (TOF) measurements. In this type of measurement, the time it takes the neutron to travel from the target to the detector is related to its velocity, which in turn is related to its kinetic energy. To determine the initial start time, a short beam pulse, of about 3 ns, can be used to restrict the possible start times. The stop time for the neutron TOF is then determined by the detector. Gamma rays and neutrons can be distinguished by their different TOFs, so that it is not necessary to have a detector that is inherently only sensitive to neutrons. It is also important that the detector provide good time resolution, similar to the beam width, when it detects a particle. To provide good separation between the neutrons and gamma rays, as well as to improve the neutron energy resolution, long separations (~2 m) between the target and detector are required. These long drift distances from target to detector also place an importance on a large surface area detector. Given these requirements of fast timing and large area, polyvinyl toluene (PVT) scintillator is a natural choice for a detector.

The detectors should have several features based on experience conducting similar measurements. There should be two photomultiplier tubes (PMTs), one on either end, to determine the time and position information of the neutron hit. There should be a nominal amount of lead in front of the scintillator to shield from lower energy gamma rays. Borated polyethylene should be placed around the sides and back of the detector for shielding of the detector.

The intrinsic detector efficiency is based on very similar measurements conducted at the Idaho Accelerator Center (IAC). The experiment was measurements on neutron correlation in photofission on ^{238}U. Plastic scintillators with an active volume of 76.2 cm x 15.2 cm x 3.8 cm were used to conduct TOF measurements. An estimated intrinsic efficiency from these measurements is 4%.

This same measurement provides guidance for target-detector distance to provide adequate separation of the neutrons and gamma rays in the TOF spectra. These measurements, which had a target-detector distance of 125 cm, show photon-related signal out to 50 ns with respect to the gamma rays in the TOF. If the maximum neutron energy is approximately 7 MeV, then a 200 cm drift distance is adequate to provide the 50 ns separation between the gamma rays and the neutrons in the detector.

2.3.2 Delayed Neutrons

For the delayed neutrons, absolute detector efficiency is critical because of the relatively weak signal strength, whereas the timing of the event is not. Furthermore, to limit background, it will be important to strongly distinguish between neutrons and gamma rays, so that some inherent neutron/gamma discrimination capability is important. Finally, we want to detect as broad a range in energy of neutrons as possible. Given these constraints, we recommend using moderated ^{3}He detectors for the delayed

neutrons. Liquid scintillators are a second option, but the intrinsic energy threshold of liquid scintillators for neutrons of about 1 MeV suggests that it would not be the ideal detector medium. That said, the ability to place liquid scintillators close to the target to improve solid angle coverage is an attractive option that may prove necessary if adequate rates cannot be achieved with moderated ^{3}He detectors.

The intrinsic neutron detection efficiency is based on discussions in (Kouzes et al. 2008). This paper cites an intrinsic efficiency of 5.4% for ^{252}Cf neutrons. The detector consists of a single ^{3}He tube with an internal diameter of 49.9 mm and a length of 1.83 m filled with 3 atmospheres of gas. The detector is surrounding by 5 cm of polyethylene, with an outer dimension of 62 cm by 201 cm. The stated efficiency is for neutrons striking the surface of the moderator. For the experimental counting rates, we assume a moderated detector that is 30 cm x 100 cm with a single ^{3}He tube inside.

The placement of the detectors will depend on how much shielding, if any, there is surrounding the detectors. For the delayed products, there is no preferred angle for emission, so the placement of the detectors is driven more by covering the needed solid angle then by examining potential angular dependence; although there may be some angular dependence for the large DU target. A potential design for the detector arrangement, including for delayed photons, is shown in Figure 2 with a target-detector distance of 55 cm. In this figure, 4" of shielding is placed around the detectors, together with a 4" long collimator opening toward the target. It is not recommended to combine the delayed neutron and delayed photons measurements into one measurement as they require significantly different beam structures. As in the figure, we assume six delayed neutron detectors.

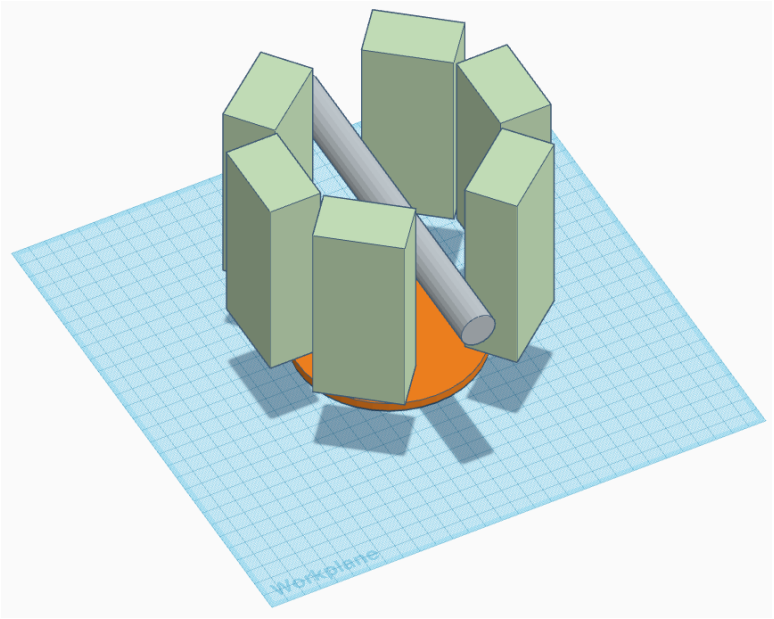

Figure 2. Concept for detector layout for the delayed neutron measurement. The green blocks are the shielded moderated ^{3}He detectors. The gray cylinder represents the beam path. The orange disk has a radius of 55 cm.

2.3.3 Delayed Photons

The delayed photons are considerably more numerous compared to the delayed neutrons, ~7 per fission compared to ~0.01 per fission, respectively, so that solid angle coverage is not as important. However, there is a need to distinguish photons with energy greater than 3 MeV, thus some energy resolution is required. Fast timing of the scintillators is not critical, since these are delayed products. NaI(Tl)

detectors will serve these purposes adequately. We assume four 4" x 4" x 16" NaI(Tl) detectors. We also assume a modest 4" collimator on the opening of the shielding. A possible configuration for the delayed photon setup is shown in Figure 3 with a target-to-detector distance of 40 cm; the front of the collimator is 30 cm from the target. Note that differences in the beam structure for the delayed photons and delayed neutrons, as discussed in section 2.4, suggest that they cannot be run efficiently at the same time.

We estimate the peak efficiencies of these detectors using charts found in (Knoll 2010). Figures 10.24 and 10.25 in this reference show the total detection efficiency and peak-to-total ratio for various thicknesses of NaI(Tl) as a function of photon energy. If we approximate the average delayed photon energy as 1.3 MeV and the average delayed photon with at least 3 MeV as 4 MeV, the total efficiency is approximately 80% and 75% at 1.3 and 3 MeV, respectively, for 10 cm of NaI(Tl). The peak-to-total ratio is 36% and 17% at these two energies, respectively, so that we approximate the peak detection efficiency as 29% for all delayed photons and 13% for delayed photons with energies greater than 3 MeV.

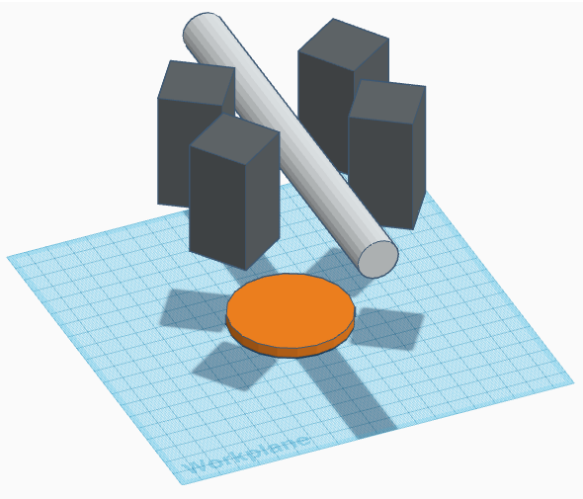

Figure 3. Concept for detector layout for the delayed neutron measurement. The black blocks are the NaI(Tl) detectors. The gray cylinder represents the beam path. The orange disk has a radius of 30 cm.

2.4 Beam Parameters

To optimize the measurements, measurements for each detected particle (prompt neutron, delayed neutron or delayed photon) should have its own beam parameters. These parameters include repetition rate of the pulses, pulse width (in time), peak current of the pulse, and possibly some macro structure allowing for long periods without any beam to address delayed products. These parameters are discussed for each of the measurements below. The effective average beam current for estimating measurement times for various measurements is shown in Table 4.

Table 4. Effective average beam current for the various measurements

Particle	I [nA]
Prompt Neutrons, 10 g target	790
Prompt Neutrons, 1,000 g target	32
Delayed Neutrons, Train = 10 s	330
Delayed Neutrons, Train = 100 s	1,900
Delayed Photons, Train = 10 s	21
Delayed Photons, Train = 100 s	200

2.4.1 Prompt Neutrons

The intensity of prompt neutrons, compared to delayed neutrons, is approximately 200 to 1, which implies that it is not necessary to address the potential contributions from delayed neutrons when measuring prompt neutrons since we are concerned with measurements uncertainties of approximately 5%. The limitation on the rate of measuring prompt neutrons is typically the maximum repetition rate of the accelerator. Another important constraint is that the length of the beam pulse should be short, ~3 ns, since we plan on conducting TOF measurements. For instance, if the start and stop times have an uncertainty of 3 ns each and the target-detector distance is 200 cm, then the uncertainty in the neutron energy is 0.06 MeV and 1 MeV at 1 and 7 MeV, respectively.

Guidance on appropriate beam parameters is provided by a recent experiment at the IAC measuring correlated neutrons from photofission on DU. The measurement involved an 8 g sample of DU. The detectors, which are the same size as used for the count rate estimates above, were placed at 125 cm from the target. The beam was tuned to provide approximately 0.5 fission per pulse in order to minimize possible uncorrelated fissions in the measurement. This restriction is not critical for these measurements, but we will use the same beam parameters as the correlation measurement to be conservative in our count rate estimates. To match the recent experiment, the chosen beam parameters for the 10 g targets are a repetition rate of 240 Hz, a pulse width of 3 ns, and a peak current of 1.1 A. For the 1,000 g DU target, we use the same parameters but scale the peak current; the peak current is reduced by a factor of 100 to account for the additional mass and is increased by the square of the ratio of the distances of the detectors for the proposed measurement and the completed measurement.

2.4.2 Delayed Neutrons

The time dependence of the delayed neutrons differs for ^{235}U and ^{238}U, see Table 5. As a result, the approach in the proposed standard is to consider different integration times, all starting at 1 ms after a beam pulse to 0.1, 1 and 10 seconds. The differences in the time dependence between the two isotopes requires different surrogate approaches for different integration times.

Table 5. List of delayed neutron time grouping parameters from (Kull et al. 1970). The relative abundances as measured at 8 and 10 MeV were averaged to approximate the abundance at 9 MeV.

$t_{1/2}$ [s]	Rel. Abundance	
	^{235}U	^{238}U
0.3	0.035	0.100
0.6	0.085	0.181
2	0.346	0.364
5	0.221	0.168
20	0.256	0.164
55	0.057	0.023

This consideration of the delayed neutron strength over an integration time after a single beam burst is too simplified when considering how these measurements are likely to be conducted. With the relatively low multiplicity of ~0.01 delayed neutrons per fission and a relatively short time scale in which to detect SNM of ~100 s, it is quite likely that an implemented active interrogation system utilizing delayed neutrons will try to create as many fissions as possible by exposing the interrogated object to as much beam as possible, while looking for delayed neutrons between beam bursts. Thus, the time dependence of the delayed neutrons becomes critical when looking at how long the interrogated object is exposed to beam. For instance, the longer delay times will play a more important role if the object is exposed to longer periods of beam.

We propose to change how the relative strengths of DU and HEU for delayed products are integrated over time for the proposed standard. The standard currently counts the delayed products (neutrons or photons) over a period of time after a single beam burst. This simple measurement approach, however, is unlikely to provide the necessary counts for the delayed products unless there is a dramatic increase in the beam intensity. To improve the standard to better reflect how measurements are likely to be conducted, we propose to count the delayed products between beam bursts while the interrogated objected is exposed to beam pulses over a period of time, e.g., 10 or 100 seconds. The proposed validation measurements for delayed neutrons and photons reflects this change.

The delayed neutrons from photofission are produced out to a few hundred seconds after the fission according to Kull et al. (Kull et al. 1970). However, the maximum reasonable measurement time for cargo screening is 100 seconds. Thus, if the object is exposed to beam for 100 s, there will be significant delayed neutrons produced after the beam is turned off. If one waits twice the maximum half-life of the time groups, 110 seconds, then less than 1% of the counts observed during the 100 second train of beam pulses is produced by previous trains. For this reason, we propose to use a macro structure to the beam, which begins with a train of pulses at the beginning, followed by a long time to allow the delayed products to decay, as shown in Figure 4.

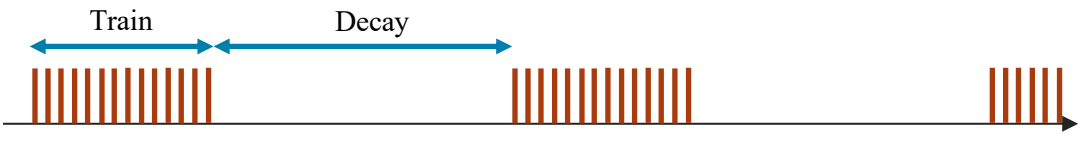

Figure 4. Diagram of beam macro structure consisting of a train of pulses followed by a long decay time

For the delayed measurements, we will use the available parameters for the linear accelerator at the University of Michigan. This accelerator can provide pulses up to 4 μs in width with peak currents of 100

mA. We assume a repetition rate of 10 Hz and consider pulse train lengths of 10 and 100 seconds, with 110 second decay time.

2.4.3 Delayed Photons

We were unable to identify references measuring the full time dependence on the delayed photons from photofission. (Walton et al. 1964) is the only reference that provides some time dependence information for both ^{235}U and ^{238}U, but it goes out to only 7 seconds. In contrast, the longest time component for delayed neutrons from neutron-induced fission is 940 seconds, so that there is significant time domain missing from the Walton et al. paper. (Gozani 2009) also mentions that the time components for delayed photons from photofission is considerably longer than for delayed neutrons. For these reasons, we use the neutron induced time dependent groupings found in (Reilly et al. 1991) as an imperfect proxy. The time groupings are presented in Table 6.

Table 6. List time grouping parameters for delayed photon from neutron-induced fission from (Reilly et al. 1991).

$t_{1/2}$ [s]	Rel. Abundance	
	^{235}U	^{238}U
0.29	0.011	0.062
1.7	0.166	0.203
13	0.304	0.324
100	0.274	0.233
940	0.245	0.279

The long half-lives of the time components suggest that it will be necessary to have an extended decay time. As with the delayed neutrons measurements, a decay time of twice the maximum half-life of the time group would reduce the contributions from previous pulse trains to less than 1% in a pulse train; thus, we recommend a decay length of 1880 seconds. Once background contributions are considered, it is likely that a shorter decay length can be used. For the other beam parameters, we use the same as for the delayed neutron measurement, based on the University of Michigan facility; namely 4 μs pulse width, 100 mA peak current, 10 Hz repetition rate with pulse trains of 10 and 100 seconds.

2.5 Multiplicities

The multiplicities are defined as the number of particles emitted per interaction. For (γ, n) the multiplicity is one for prompt neutrons and zero for all other particles. For fission, the total number of prompt neutrons is determined from ENDF/B-VII.1 (Chadwick et al. 2011) for photofission at 8 MeV, the approximate maximum of the product of the bremsstrahlung photon energy distribution and the fission cross section: 2.7 and 2.8 neutrons per fission for HEU (93% ^{235}U) and DU (100% ^{238}U), respectively. The total yield for delayed photons is taken from the total yield of delayed photons from neutron induced fission in (Reilly et al. 1991), while the total yield for delayed neutrons is taken from (Caldwell and Dowdy 1975). The total number of particles per fission are shown in Table 7.

Many of the observables studied require additional cuts, either in time or energy. For the prompt neutrons, the fraction of neutrons above a given neutron energy threshold is determined through MCNP6 version 1.0 (Goorley et al. 2011). For the delayed products, the strength for all delayed particles is determined using a code which aggregates the delayed response over multiple pulses and then integrates

over the appropriate time. For delayed photons with energy greater than 3 MeV, the number of delayed photons per fission with energy above 3 MeV from (Gozani 2009) is divided by 7, the approximate total number of delayed photons. The resulting product of the total multiplicities in Table 7 and the fraction of particles in Table 8 is then used as the "multiplicity" ν in the count rate estimate.

Table 7. Multiplicities for all particles of specific type from photofission

Particle	HEU	DU
Prompt Neutrons	2.7	2.9
Delayed Neutrons	0.011	0.029
Delayed Photons	6.5	8.7

Table 8. Fraction of products from fission for various situations

Particle	Description	^{235}U	^{238}U
Prompt Neutrons	All E	1.00	1.00
	E > 1 MeV	0.52	0.36
	E > 3 MeV	0.13	0.082
Delayed Neutrons	Train = 10 s	0.51	0.63
	Train = 100 s	0.87	0.92
Delayed Photons	Train = 10 s, All E	0.22	0.30
	Train = 100 s, All E	0.51	0.60
	Train = 10 s, E > 3 MeV	0.0041	0.0047
	Train = 100 s, E > 3 MeV	0.0095	0.0093

2.6 Count Rates

The estimated counting rates following Eqn. (1) are calculated with the detailed information tabulated above. The goal is for a 3.5% uncertainty measurement for each material, so that the ratio of the response has a 5% uncertainty. If we assume a signal-to-noise ratio of 1, then we will require 1600 counts in the detector to achieve 3.5% (statistical only) uncertainty after the background subtraction. For the delayed photons with energies greater than 3 MeV, we assume that there is no background so that 820 counts are required to achieve the 3.5% uncertainty. Table 9 summarizes the count time in hours required to achieve this objective. With a few notable exceptions, most the counting times are in the range of a few hours. The longest count times are for delayed photons with energies greater than 3 MeV. The estimated time for these measurements is long, approximately two weeks, but not unreasonable. Also note that all of the different energy ranges for prompt neutrons and delayed photons are conducted simultaneously, so that the E > 3 MeV counting essentially determines the required beam time.

Table 10 shows the total beam time in hours calculated for each experiment. Several considerations need to be addressed to translate the estimated counting times in Table 9 into total beam time required. First, there is generally some beam tuning period required to get the beam properly adjusted. We will assume 8 hours per setup (4 hours for the test run and 4 hours for the production run). Second, a test run is necessary to resolve experiment issues. We assume 16 hours for the test run. The test run should be conducted a few weeks before the production run if possible, in order to allow time for the issues to be resolved. Third, there is generally an assumed macroscopic efficiency factor of 50%, which addresses

machine and equipment down time as well as time for room accesses to change targets, for example. For the delayed neutrons with a 10-s pulse train length, we increased the targeted statistical uncertainty from 3.5% to 5% in order to reduce the measurement time. Finally, the minimum measurement time is 2 hours, regardless of the required count time.

Table 9. Counting time in hours to achieve 3.5% statistical uncertainty with a signal-to-noise ratio of 1

	HEU, 10 g	DU, 10 g	DU, 1 kg
Prompt Neutrons			
All E	3.0	2.9	1.1
E > 1 MeV	5.9	8.1	3.2
E > 3 MeV	23	35.5	14
Delayed Neutrons			
Train = 10 s	33	14.2	0.1
Train = 100 s	3.4	1.7	0.0
Delayed Photons, All E			
Train = 10 s	1.9	1.4	0.0
Train = 100 s	0.1	0.1	0.0
Delayed Photons, E > 3 MeV			
Train = 10 s	120	100	1.0
Train = 100 s	5.2	5.3	0.1

Table 10. Estimated beam time in hours for conducting the validation measurements

Experiment	Beam Tune	Test Run	Production Run			Total Time
			HEU, 10 g	DU, 10 g	DU, 1 kg	
Prompt Neutrons	8	16	46	70	28	168
Delayed Neutrons, Train = 10 s	8	16	66	28	2	120
Delayed Neutrons, Train = 100 s			7	4	2	13
Delayed Photons, Train = 10 s	8	16	60	50	2	136
Delayed Photons, Train = 100 s			10	10	2	22

3.0 Cost Estimates

There are several items that contribute to the estimated cost of the validation experiments. These include costs to develop detector systems, modify data acquisition systems, fabricate the targets, data analysis and travel. The rough order-of-magnitude costs estimate per institution are shown in Table 11. It is envisioned that this effort will take three years, with approximately constant spending each year, except for the second year when the $100k for the beam time at Idaho State would be necessary. In summary, the total rough order-of-magnitude cost estimate to conduct all three (delayed photon, prompt neutron, delayed neutron) of the photofission measurements is $1.1M.

There are several critical assumptions in estimating these costs:

- PNNL will fabricate the 10 g HEU and 10 g DU target so that they have similar geometry.
- The detector materials are available but may need to be reconfigured to be suitable for these measurements.
- Shielding and structural materials for the experimental setup are available.
- The prompt neutron measurements will be conducted at the IAC, while the delayed neutron and photon measurements will be conducted at the University of Michigan.
- A large sample of DU, in the range of 1 kg, is available at both experimental facilities.
- Students at the facilities will be involved in the experimental design, setup, testing, production, analysis and reporting.

Table 11. Summary of rough-order-of-magnitude cost estimate for measurements broken down by institution

Institution	Labor	Beam Time
PNNL	$400k	
Idaho State	$300k	$100k
University of Michigan	$300k	

4.0 Summary

The proposed standards for active interrogation of cargo containers considers possible measurement methodologies related to photofission, differential die-away and nuclear fluorescence. Of these methodologies, the approach that currently carries the most interest is photofission, so that the design of the validation measurements considers the various possible products that could be measured from photofission: namely prompt neutrons, delayed neutrons and delayed photons.

There is a limited range of facilities in the U.S. that have both the necessary accelerator capability and the ability and willingness to handle SNM. Two such facilities, the Idaho Accelerator Center at Idaho State University and the Nuclear Engineering Program at the University of Michigan, have both expressed an interest in participating in these measurements. Both would need to amend their licensing to handle the 10 g of HEU proposed for these measurements; the licensing has minimal impact on cost but potentially a significant impact on schedule.

The rough order-of-magnitude cost estimate for all three validation measurements is $1.1M, spread over three years. Each of the three measurements could be performed separately, at approximately one-third of that cost. There are a number of critical assumptions in these cost estimate that will need to be confirmed before a final cost estimate can be established.

For the validation measurements, PNNL will manage the research effort to ensure that the overall objective of the validation measurements can be achieved, while much of the labor is provided by the two collaborating universities as research opportunities for students. PNNL will also prepare the two 10-g targets. The successful completion of these validation measurements would reduce the uncertainties in the standards from about 50% to 5%. The measurements would also provide some much-needed nuclear data on photofission.

5.0 References

Agostinelli, S, et al. 2003. "GEANT4-a simulation toolkit." *Nuclear Instruments & Methods in Physics Research Section a-Accelerators Spectrometers Detectors and Associated Equipment* 506(3):250-303. https://doi.org/10.1016/s0168-9002(03)01368-8.

Allison, J, et al. 2006. "Geant4 developments and applications." *Nuclear Science, IEEE Transactions on* 53(1):270-78. https://doi.org/10.1109/TNS.2006.869826.

Caldwell, JT, and EJ Dowdy. 1975. "Experimental Determination of Photofission Neutron Multiplicities for 8 Isotopes in Mass Range 232 ≤ A ≤ 239." *Nuclear Science and Engineering* 56(2):179-87.

Chadwick, MB, et al. 2011. "ENDF/B-VII.1 Nuclear Data for Science and Technology: Cross Sections, Covariances, Fission Product Yields and Decay Data." *Nuclear Data Sheets* 112(12):2887-996. https://doi.org/10.1016/j.nds.2011.11.002.

Goorley, T, et al. 2011. *Initial MCNP 6 Release Overview*. Report No. LA-UR-11-07082, Los Alamos National Laboratory, Los Alamos, New Mexico.

Gozani, T. 2009. "Fission Signatures for Nuclear Material Detection." *Ieee Transactions on Nuclear Science* 56(3):736-41. https://doi.org/10.1109/Tns.2009.2015309.

Knoll, GF. 2010. *Radiation Detection and Measurements*. 4th ed., John Wiley, New York.

Kouzes, RT, et al. 2008. "Passive neutron detection for interdiction of nuclear material at borders." *Nuclear Instruments & Methods in Physics Research Section a-Accelerators Spectrometers Detectors and Associated Equipment* 584(2-3):383-400. https://doi.org/10.1016/j.nima.2007.10.026.

Kull, LA, et al. 1970. "Delayed Neutrons from Low Energy Photofission." *Nuclear Science and Engineering* 39(2):163-+.

Reilly, D, N Ensslin, and H Smith, Jr. 1991. *Passive Nondestructive Assay of Nuclear Materials*. Report, Los Alamos National Laboratory, Los Alamos, New Mexico.

Walton, RB, et al. 1964. "Delayed Gamma Rays from Photofission of U-238, U-235, and Th-232." *Physical Review* 134(4B):B824-B32.

Pacific Northwest
NATIONAL LABORATORY

www.pnnl.gov

902 Battelle Boulevard
P.O. Box 999
Richland, WA 99352
1-888-375-PNNL (7665)

U.S. DEPARTMENT OF
ENERGY